# Comparison Between Graphene Oxides Reduced by Microwave System with Different Power Sets

*A.L.B. S. Martins[a]\* , E.F. da Silva[b] , M.F.V. Marques[c], W.A. Pinheiro[a]*

*[a]Instituto Militar de Engenharia, Seção de Engenharia de Materiais, Urca, Rio de Janeiro, RJ, Brasil.*
*[b]Universidade Federal do Rio de Janeiro, Laboratório de Ensaios Não Destrutivos, Corrosão e Soldagem, Rio de Janeiro, RJ, Brasil.*
*[c]Universidade Federal do Rio de Janeiro, Instituto de Macromoléculas, Rio de Janeiro, RJ, Brasil.*

The present work compares graphene oxides produced by the Marcano's method and the subsequent reduction process using a microwave system with different power and time sets. The thermal profiles of the reduction processes were analyzed, emphasizing the heat capacity from the 600 W test of 3.44 kJ/K. The X-ray diffraction showed a reduction in the interlayer space and the number of layers in all powers. The infrared and UV-Vis spectroscopy results showed a clear decrease in the bands corresponding to the oxygenated group and partial restoration of aromatic bonds. The Raman spectroscopy showed that the 1000 W power set originated a higher defective structure. The observed results allow the conclusion that the 600 W power promotes a little better result between the analyzed power sets.

**Keywords:** *graphene oxide; microwave reduction; X-ray diffraction; FTIR.*

## 1. Introduction

Although graphene constitution has been theoretically known for decades, it was only in 2004 that a group of scientists led by Geim and Novoselov found graphene in its isolated monolayer form. The feat was carried out using a technique of successive mechanical exfoliations with adhesive tape, providing an easy route to obtain this type of material, which earned the two scientists the Nobel Prize in Physics in 2010[1,2]. Since then, studies in the graphene area have experienced an incredible expansion in the most diverse application areas: thermal, electrochemical, multifunctional composites, appropriate composites, mainly due to its excellent electrical and thermal conduction properties and high optical transmittance and stiffness modulus[3,4].

However, producing graphene in its purest form and separating it has been a great challenge, mainly because the routes do not have industrial scalability. This fact has led several scientists to seek production alternatives[4-6]. Among the various forms of graphene production and its derivatives, one of the most common approaches and the only one considered viable on a large scale consists of the production through intercalation and oxidation of graphite by strong oxidizing agents[7], followed by reduction. In partnership with Prof. Tour, Daniela Marcano, both at Rice University – USA, developed a method using sulfuric acid, phosphoric acid, and potassium permanganate in oxidation. According to the authors, this method provides a safe route due to the inhibition of the production of toxic gases. In addition, it promotes more intact basal structures of the graphene oxide (GO) lamellae without loss of reaction productivity[7].

After the intercalation and oxidation, the reduction step is carried out, which consists of restoring the conjugated π bonds and partial release of the oxygenated groups. According to Shang et al.[8], there are three main reduction processes: thermal reduction, chemical reduction, and electrochemical reduction. Each type of reduction provides the driving force for the reduction through temperature, chemical potential, and electrical current, respectively, creating end products with different characteristics.

The thermal reduction is the one that presents the best cost-benefit, despite the long duration periods[8]. In an attempt to optimize processing time, several studies have used microwave-assisted reduction as a solution to speed up the thermal reduction of graphene oxides[9,10]. Microwave radiation promotes the reduction both by heating the medium and by the dielectric properties of graphene oxide, which result in preferential absorption of radiation over solvent without losing the quality of the final product[10].

The choice of a proper solvent in a solvent-assisted microwave reduction significantly influences the final properties of the reduced graphene oxide. Tien and coworkers, in their work, showed that the use of methyl-pyrrolidone as an organic solvent during graphene oxide reduction leads to the higher carbon content in the final chemical composition due to the presence of amide groups and the creation of free radicals that significantly enhance the deoxygenation of graphene oxide[11]. In his review article, Jakhar *et al.* also showed that the choice of the parameters leads to different properties on the final microstructure and is just an important factor as the choice of the oxidation route[9,10].

The present work aims to evaluate the influence of kinetic effects on the reduction of graphene oxides dispersed

in n-methyl-pyrrolidone and water solution by microwave irradiation, using different power and time sets, through the techniques of X-ray diffraction, infrared spectroscopy, UV-Vis spectroscopy, Raman spectroscopy, and temperature profile during the reduction process.

## 2. Materials and Methods

### 2.1. Materials

The following materials were used in the preparation of the reduced graphene oxides:
- commercial graphite, Graflake 99850, from Nacional de Grafite;
- sulfuric acid ($H_2SO_4$), 98%;
- phosphoric acid ($H_3PO_4$), 35%;
- potassium permanganate ($KMnO_4$), 99%;
- hydrogen peroxide ($H_2O_2$), 30%;
- hydrochloric acid (HCl), 37%;
- ethanol, 96%;
- n-methyl-pyrrolidone (NMP), 99%.

All the materials used were of reagent grade and were used as received, without further purification procedures.

### 2.2. Methods

The preparation of graphene oxide was carried out as predicted by Marcano et al.[7,12] A brief description of the method follows. First, 360 mL of sulfuric acid ($H_2SO_4$) and 40 mL of phosphoric acid ($H_3PO_4$) were added to 3 g of graphite (Graflake 99550) purchased from the Brazilian company Nacional de Grafite. After 30 min of stirring, 18 g of potassium permanganate ($KMnO_4$) were slowly added to the mixture, and the 12 h oxidation process was driven at 50 °C. After oxidation, the material was poured onto 400 mL of ice and dripped with 10 mL $H_2O_2$. The material was allowed to settle for two days. Next, the intercalated graphite was washed with a 600 mL of a solution composed of 200 mL of ethanol, 200 mL of double-distilled water, and 200 mL of HCl 30% solution. Then, the material was centrifuged at 7500 rpm, at 25 °C, for 45 min using the Eppendorf 5430 centrifuge. After centrifugation, the graphene oxide (GO) produced was diluted in 1 L of double-distilled water, resulting in a 5.9 mg/mL final concentration.

An Anton-Paar Microwave 3000 continuous microwave reactor was used in the microwave reduction. 140 mL of the GO solution was diluted in 360 mL of NMP and stirred for 30 min to total homogenization achieving a final concentration of 1.652 mg/mL of reduced graphene oxide (RGO). To study possible differences and kinetic effects, similar energies were delivered to the dispersion of graphene oxide in n-methyl-pyrrolidone (GO + NMP) but with different energy delivery rates (power sets). The following power and time ratios were used to limit the final temperature of the system to 75% of NMP boiling point and simultaneously deliver a similar total energy amount: 600 W and 700 s, 800 W and 520 s, and 1000 W and 420 s. No additional pressure or inert atmosphere was used.

The samples produced in this work were characterized by X-ray diffraction (Shimadzu - XRD-7000), using a Cu Kα radiation source (λ = 0.1542 nm), a voltage of 40 kV, a current of 30 mA, and a scan speed of 0.5 deg/min from 7 to 30° at room temperature and θ-2θ coupled mode. The XRD samples were deposited over a monocrystalline silicon substrate using a vacuum chamber at room temperature. Fourier-Transform Infrared-Photoacoustic Spectroscopy – FTIR-PAS (Thermo Scientific - Nicolet 6700 with photoacoustic cell MTEC 100) analyses of the samples were carried out with 256 scans averaged in a range from 4000 cm⁻¹ to 500 cm⁻¹, a gain of 3, resolution of 16 cm⁻¹, and helium gas purge flow of 5 mL/min. The reference spectrum used was pressed activated charcoal. UV-Vis spectra (Thermo Scientific - Evolution 200) of isopropyl alcohol dispersions of GO and RGO were acquired with a concentration of 0.5 mg/mL, in quartz cuvettes, with a scan rate of 1 nm/min from 700 nm to 200 nm at room temperature; Raman spectra of the samples were obtained with a confocal Raman microscope (Bruker - Senterra) using the 532 nm laser excitation, with power set to 2 mW, integration time of 10 seconds in the spectral range from 1000 to 3000 cm⁻¹. The laser beam was focused on the sample with a 100× long-working distance objective, and the resolution was set to 3 to 5 cm⁻¹. The samples were deposited over a monocrystalline silicon substrate using a room-temperature vacuum chamber. Temperature profiles were built using a K-type thermocouple (Chromel/Alumel) from Wärme do Brasil. The measurements were taken in regular steps of 30, 40, and 50 seconds and the macro aspects of reduction evolution were also registered with a cellphone camera.

## 3. Results and Discussion

Graphs with temperature surveys and macro-optical observation of the sample throughout the reduction process are displayed in Figure 1.

The first observation is the macro and color analysis of the system evolution shows that the higher power (1000 W) leads to a faster reduction, as the observed system switches from honey to black more quickly.

From the temperature surveys, it was possible to calculate the thermal capacity (C = E/ΔT) of the samples by its definition for the three sets, as well as to observe the temperature variation (ΔT) and the final temperature ($T_f$) of the system. The total amount of energy delivered (E) by the power set of 800 W was limited to 416 kJ to keep the final temperature close to 151° C, as stated in methods, as well as equipment limitations. The results are shown in Table 1.

Even though the amount of energy in the three systems was not the same, the heat capacity results allow us to normalize this parameter, showing that the presence of GO increases the expected value for the NMP + water mixture (1.34 kJ/K), which can be explained by the preferential absorption of microwave radiation by the GO[10]. There was a greater heat capacity when the power of 600 W was used, which can indicate greater energy absorption by the graphene oxide reduction process.

Three samples of each GO and RGO (reduced graphene oxide) product were analyzed by X-ray diffraction. As shown in Figure 2, the peak of graphene oxide relative to the (002) on 2θ = 9.7° for GO and peak values of (002) of the reduced graphene oxide samples around 25° were positioned just as expected in the literature[13]. The RGO peaks were at angles close to the Graflake, as expected when the reduction process
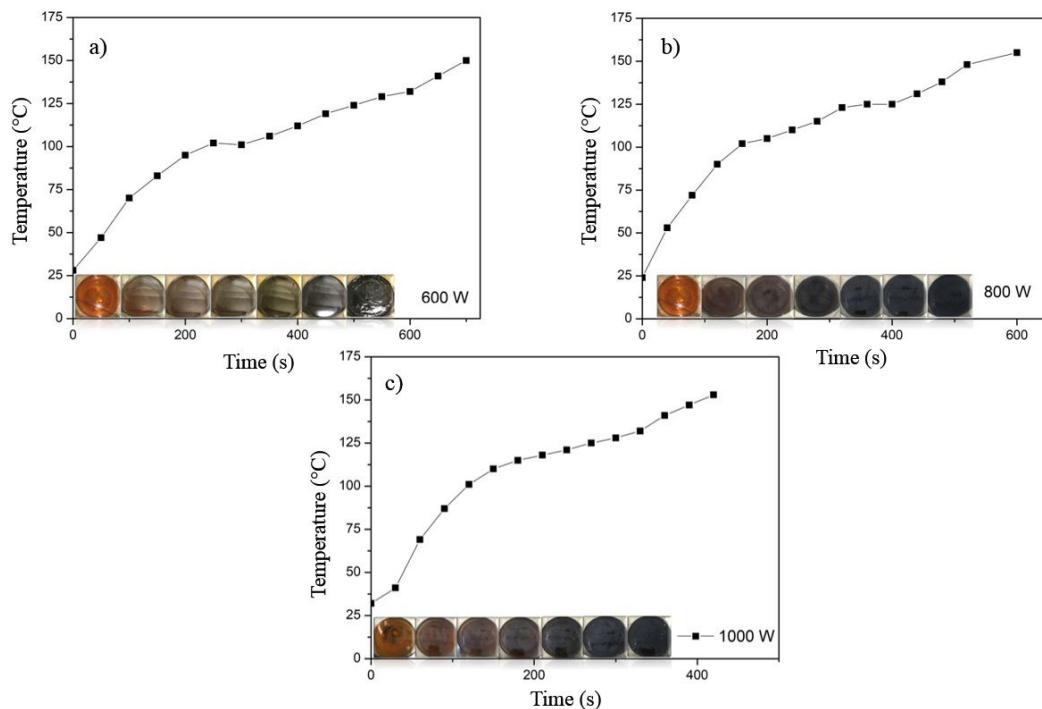
**Figure 1.** Heating tracking graphs of n-methyl-pyrrolidone and graphene oxide (NMP + GO) dispersion for different powers: (a) 600 W; (b) 800 W; and (c) 1000 W.
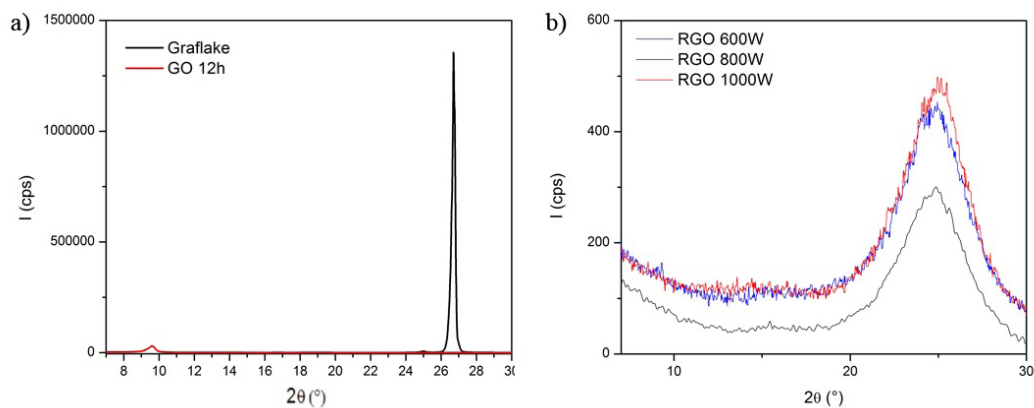


**Figure 2.** X-ray diffractograms of (a) graphite as received and GO; (b) RGO produced with different microwave reduction time and power parameters.

**Table 1.** Final temperature and heat capacity.

| Material | $T_f$ (°C) | E (kJ) | ΔT (K) | C (kJ/K) |
|---|---|---|---|---|
| NMP + Water + RGO - 600 W | 150 | 420 | 122 | 3.44 |
| NMP + Water + RGO - 800 W | 153 | 416 | 126 | 3.30 |
| NMP + Water + RGO - 1000 W | 153 | 420 | 123 | 3.41 |

occurs, which is associated with the return of the interplanar distance before oxidation, as will be detailed as follows.

From the diffractograms, the interplanar spacings ($d_{002}$) were calculated by Bragg's law, the crystallite sizes ($L_{002}$) were calculated by the Scherrer equation, and the number of layers (N) by Equation 1[14]. The results are expressed in Table 2.

$$L_{002} = (N_1 - 1).d_{002} \qquad (1)$$

where $N_1$ is the number of layers, $L_{002}$ is the crystallite size in the dimension perpendicular to the plane of the graphene sample, $d_{002} = \lambda/(2\sin\theta)$, with $\lambda = 1.54$ nm as the wavelength of the X-ray, and $\theta$ is the angle between the incident X-rays and diffracting crystal planes.

**Table 2.** Interlayer distance ($d_{002}$) and the number of layers (N).

| Material | $\theta$ (°) | $L_{002}$ (nm) | $N_1$ | $d_{002}$ (nm) |
|---|---|---|---|---|
| Graflake | 26.6 | 40.773 | 123.3 | $0.335 \pm 0.001$ |
| GO | 9.7 | 6.984 | 9.2 | $0.896 \pm 0.010$ |
| RGO 600 W | 24.8 | 2.104 | 7.1 | $0.352 \pm 0.003$ |
| RGO 800 W | 24.5 | 2.193 | 6.4 | $0.362 \pm 0.002$ |
| RGO 1000 W | 24.8 | 1.981 | 6.6 | $0.355 \pm 0.001$ |

The crystallite size of the samples decreases with the process of obtaining GO and even more with the reduction, which can be associated with the process of exfoliation of the layers. Furthermore, with oxidation, the interplanar distance is greater in GO due to the presence of oxidized groups. It falls with reduction to a distance very close to that of graphite, indicating the efficiency of removing oxidized groups. It was also observed with 95% confidence that the greatest reduction in the interplanar distance was obtained with the sample reduced with 600 W of power than the GO samples (60,7% decrease), indicating a greater elimination of oxygenated groups[15].

As shown in Figure 3, the FTIR spectra show that all samples presented a spectrum similar to Graflake with the complete reduction in the OH band, around 3400 cm[-1][7]. There was also partial reconstruction of the aromatic C=C band, around 1500 cm[-1][7,16], being more pronounced in the 600 W sample, as well as the appearance of the C=C conjugated band around 2350 cm[-1][16]. It is possible to observe that there is still a residual C=O band around 1700 cm[-1][17] in the materials obtained at the powers of 800 W and 1000 W. These results are in agreement with the analysis of the interlayer space, showing that the sample 800 W has the worst oxygenated groups removal and the sample 600 W has the best removal of oxygenated groups.

In the UV-Vis spectra, as shown in Figure 4, the reduction process occurred at all powers, as shown by the appearance of the band relative to the $\pi$-$\pi$* transitions at 230 nm. The spectra also show the reduction of the intensity of the band around 280 nm, assigned to the n-$\pi$* of the C=O group transitions[7,15], with a more significant decrease for the GO reduction process carried out using 600 W of power and a more salient residual band of C=O on RGO 800 W. This result is in agreement with those obtained by FTIR and X-ray diffraction.

Finally, the analysis of Raman spectra presented in Figure 5 shows the characteristic spectra of graphene materials, highlighting the presence of the three main signals: D band, which is associated with the degree of disorder of aromaticity (~1350 cm^{-1}); G band, related with the presence of sp[2] hybridization (~1580 cm^{-1}); and 2D band (~2700 cm^{-1}), associated to second-order process and also linked with size and stacking of graphene layers[18].

After processing the curves by Lorentzian fitting and using $\lambda_L$ as 532 nm, it was also possible to calculate the band intensities $I_D$ and $I_G$ to estimate the density of defects on the structure ($n_D$), the distance between defects ($L_D$), and the number of layers ($N_2$), according to with Cançado's Equations 3 and 4 and the results of his work[19,20]. The calculated parameters can be found in Table 3.
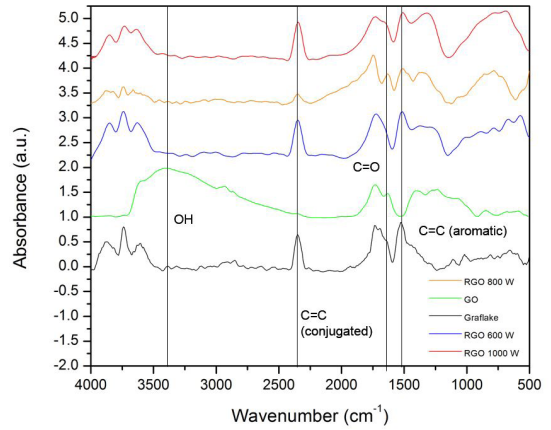


**Figure 3.** FTIR spectra of the RGOs were obtained at different powers.
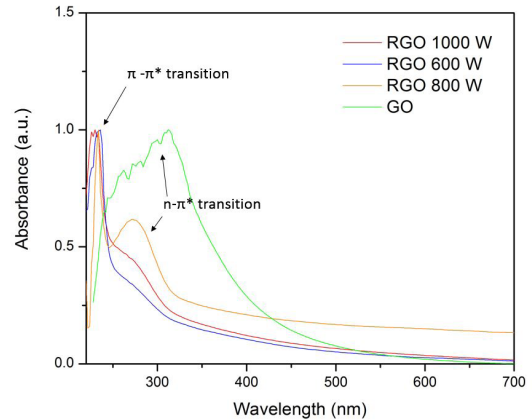


**Figure 4.** UV-Vis spectra of the materials produced.

$$L_D^2\left(nm^2\right) = (1.8 \pm 0.5) \cdot 10^{-9} \cdot \lambda_L^4 \cdot \left(\frac{I_D}{I_G}\right)^{-1} \qquad (2)$$

$$n_d\left(cm^{-2}\right) = \frac{(1.8 \pm 0.5) \cdot 10^{22}}{\lambda_L^4} \cdot \left(\frac{I_D}{I_G}\right) \qquad (3)$$

The quintuplicates average results of $I_D/I_G$ ratio and $n_D$ show that the reduction process increased the defect density in all samples compared to GO. In addition, comparing the three powers used in reduction, it is possible to observe that the RGO produced with 1000 W of power achieved the smallest $I_D/I_G$ ratio, followed by the RGO obtained with 600 W. Even though the previously characterizations have
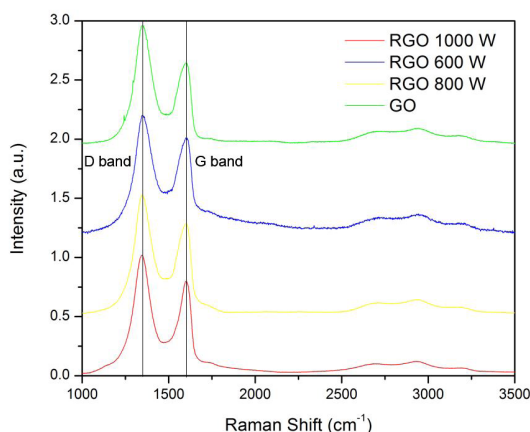
**Figure 5.** Raman spectra of GO and RGO at the different powers were analyzed.

**Table 3.** Raman spectroscopy results.

| Material | $L_D$ (nm) | N | $n_d$ ($10^{10}$ cm$^{-2}$) | $I_D/I_G$ |
|---|---|---|---|---|
| GO | 2.0 | 5 | 1019 | 1.29 |
| 800 W | 1.8 | 4 | 1248 | 1.49 |
| 600 W | 4.3 | 4 | 1092 | 1.34 |
| 1000 W | 2.0 | 4 | 1120 | 1.32 |

shown a less effective reduction for RGO 800 W samples, the Raman spectroscopy analysis showed that this power was also the more defective in terms of layer integrity. Raman analysis of the number of layers shows that RGO and GO have less than 10 layers, reaffirming the quality of the produced materials.

## 4. Conclusion

The combined results from FTIR, X-ray diffraction, UV-Vis spectroscopy, and heat capacity analyses showed that the sample RGO 600 W showed a slightly better reduction than the other powers, with a better restoration of aromatic bands, fewer oxygenated residual groups, and higher heat capacity. The RGO 800 W samples showed the worst results in terms of residual oxygenated groups as well as a higher density of defects by Raman spectroscopy analysis. It is necessary to punctuate that the results of 800 W were not performed in the same amount of energy that the other systems did due to equipment limitations and maximum temperature set. In general, these results show that, despite having received the equivalent amount of energy, the processes lead to slightly different properties, indicating that there may be a relevant kinetic component in the microwave-assisted reduction mechanism of graphene oxide.

## 5. Acknowledgment

## 6. References

1. Geim AK, Novoselov KS. The rise of graphene. Nat Mater. 2007;6:183-91.
2. Novoselov KS, Geim AK, Morozov S V., Jiang D, Zhang Y, Dubonos SV, et al. Electric field in atomically thin carbon films. Science. 2004;306(5696):666-9.
3. Collins R. Threats and opportunities for thermal interface materials content of Webinar. Cambridge: [s.n.]; 2020.
4. Collins R. Graphene, 2D materials, and carbon nanotubes 2017-2027. London: IDTechEX; 2018.
5. Ludgero M, Gomes M, Federal U, Pibic B, Matsushima JT, Espaciais P, et al. Síntese e caracterização de óxido de grafeno e / ou grafeno pelo método de oxidação química da grafite visando suas aplicações. Brasília: CNPq; 2014. Relatório Final de Iniciação Científica.
6. Vu MC, Bae YH, Yu MJ, Choi WK, Islam MA, Kim SR. Thermally conductive adhesives from covalent-bonding of reduced graphene oxide to acrylic copolymer. J Adhes. 2019;95:887-910.
7. Marcano DC, Kosynkin DV, Berlin JM, Sinitskii A, Sun Z, Slesarev A, et al. Improved synthesis of graphene oxide. ACS Nano. 2010;4:4806-14.
8. Shang YU, Zhang D, Liu Y, Guo C. Preliminary comparison of different reduction methods of graphene oxide. Bull Mater Sci. 2015;38:7-12.
9. Xie X, Zhou Y, Huang K. Advances in microwave-assisted production of reduced graphene oxide. Front Chem. 2019;7:1-11.
10. Jakhar R, Yap JE, Joshi R. Microwave reduction of graphene oxide. Carbon N Y. 2020;170:277-93.
11. Tien HN, Luan VH, Cuong TV, Kong BS, Chung JS, Kim EJ, et al. Fast and simple reduction of graphene oxide in various organic solvents using microwave irradiation. J Nanosci Nanotechnol. 2012;12:5658-62.
12. Marcano DC, Kosynkin D, Berlin JM, Sinitskii A. Correction to: Improved Synthesis of Graphene Oxide (ACS Nano (2010) 4: 8 (4806-4814). ACS Nano. 2018;12:2078.
13. Yanti DR, Hikmah U, Prasetyo A, Hastuti E. The effect of microwave irradiation on reduced graphene oxide from coconut shells. IOP Conf Ser Earth Environ Sci. 2020;456:012008.
14. Andonovic B, Grozdanov A, Paunovic P, Dimitrov AT. X-ray diffraction analysis on layers in graphene samples obtained by electrolysis in molten salts: a new perspective. Micro Nano Lett. 2015;10(12):683-5.
15. De Silva KKH, Huang HH, Yoshimura M. Progress of reduction of graphene oxide by ascorbic acid. Appl Surf Sci. 2018;447:338-46.
16. Mecozzi M, Sturchio E. Computer assisted examination of infrared and near infrared spectra to assess structural and molecular changes in biological samples exposed to pollutants: a case of study. J Imaging. 2017;3:11.
17. Iskandar F, Hikmah U, Stavila E, Aimon AH. Microwave-assisted reduction method under nitrogen atmosphere for synthesis and electrical conductivity improvement of reduced graphene oxide (rGO). RSC Advances. 2017;7:52391-7.
18. King AAK, Davies BR, Noorbehesht N, Newman P, Church TL, Harris AT, et al. A new raman metric for the characterisation of graphene oxide and its derivatives. Sci Rep. 2016;6:1-6.
19. Silva DL, Campos JLE, Fernandes TFD, Rocha JN, Machado LRP, Soares EM, et al. Raman spectroscopy analysis of number of layers in mass-produced graphene flakes. Carbon N Y. 2020;161:181-9.
20. Cançado LG, Jorio A, Ferreira EHM, Stavale F, Achete CA, Capaz RB, et al. Quantifying defects in graphene via Raman spectroscopy at different excitation energies. Nano Lett. 2011;11:3190-6.